Supplemental Modeling Information: Impact of assuming a circular orifice on flow error through elliptical regurgitant orifices: a computational fluid dynamics analysis of proximal flow convergence.

Gregory J. Wagner, Northwestern University

1 Method

1.1 Summary

The three-dimensional flow field near a finite elliptical outflow orifice was computed for a range of flow velocities, orifice sizes, and orifice aspect ratios. The flow was simulated using the open-source incompressible computational fluid dynamics (CFD) solver Nalu[1].

1.2 Flow Geometry

Only the flow upstream of the orifice was modeled, representing the converging flow field in the left ventricle during mitral regurgitation. The flow domain was modeled as a cylindrical region with a height of 10 cm and radius of 10 cm. This domain is not meant to give an accurate representation of the ventricle size or shape; rather, it was chosen to be large enough so that the form of the inflow boundary condition does not significantly affect the flow near the orifice. The axis of the cylinder is aligned with the z axis of the coordinate system. At the center of the base of the cylinder, an elliptical area represents the regurgitant orifice. The area of the orifice (A_O) and the ellipse aspect ratio are both prescribed. We simulated 3 different areas (A_O = 0.1, 0.3, and 0.5 cm^2) and 5 different ellipse axis ratios (1:1, 2:1, 3:1, 5:1, and 10:1); all 15 possible combinations were simulated.

1.3 Boundary Conditions

At the top and sides of the cylinder, the velocity is prescribed to the known far-field solution for a spherically symmetric converging flow. The total volume flow rate, Q_0, is fixed. If the center of the orifice is taken as the origin, the flow velocity as a function of radial position r can be determined by equating the total flow through a hemispherical control surface at this radius to Q_0. The resulting velocity field is

$$\mathbf{u} = -\frac{Q_O \hat{\mathbf{e}}_r}{2\pi r^2}$$

where $\hat{\mathbf{e}}_r$ is the unit vector in the radial direction. In Cartesian coordinates, this velocity is equivalently:

$$u = \frac{Q_O x}{2\pi r^3}$$
$$v = \frac{Q_O y}{2\pi r^3}$$
$$w = \frac{Q_O z}{2\pi r^3}$$

---

[1] https://github.com/NaluCFD/Nalu

where u, v, and w are the x, y, and z components of velocity, respectively. For each simulation case, the volume flow rate is prescribed to match a particular average downward velocity at the orifice (V_O); the flow rate is thus computed as $Q_O=A_OV_O$. For each geometry, three different average orifice velocities are simulated (V_O = 400, 500, and 600 cm/s), resulting in 45 individual simulations (3 orifice areas $\times$ 5 ellipse aspect ratios $\times$ 3 orifice velocities).

The inflow boundary velocity is modeled as constant in time, and the simulation is run until a steady state is reached. We verify the validity of this simplification (as opposed to pulsatile flow conditions) in Section 2.3.

The orifice area at the center of the base of the cylindrical domain is an outflow boundary condition, with a prescribed constant reference pressure of zero. The remainder of the base of the cylinder is treated as a fixed wall with no slip and no penetration (i.e., zero velocity).

1.4 Flow Model

The flow is governed by the incompressible Navier-Stokes equations for a fluid with constant density and viscosity:

$$\frac{\partial}{\partial t}(\rho \mathbf{u}) + \nabla \cdot (\rho \mathbf{u}\mathbf{u}) = -\nabla p + \mu \nabla^2 \mathbf{u}$$

$$\nabla \cdot \mathbf{u} = 0$$

In our model, blood is treated as a Newtonian fluid with density 1.05 g/cm^3 and viscosity 3.0 centipoise.

No turbulence model is used in our simulations. The maximum Reynolds number across our simulations (using the average orifice diameter as the length scale) is around 17,000. This Reynolds number is more than an order of magnitude lower at a distance of just one length scale away from the orifice. This converging, accelerating flow upstream of the orifice is very stable to perturbations and is expected to remain laminar in this range, although we are not aware of any experimental data on transition to turbulence. The fact that our simulations remain steady and stable without use of a turbulence model is strong evidence that the true flow is laminar in the simulated region. Note that our simulations do not include any part of the flow downstream of the orifice, where the flow profile would be expected to be a turbulent jet.

1.5 Computational Mesh

The 3D geometry and computational mesh for the domain were created using the commercial pre-processing software Trelis[2]. For each geometry, a mesh of quadrilateral elements was generated that was fine enough to resolve both the complex flow field near the orifice and the boundary layer at the wall. Total mesh size varied with orifice geometry, but all meshes contained between 110,000 and 190,000 elements (with the exception of a highly refined mesh used to verify mesh convergence, described in section 2.1). A typical geometry and mesh are shown in Figures 1 and 2A in the manuscript.

[2] http://www.csimsoft.com/trelis

For each geometry, the elliptical orifice is meshed with a total of 944 elements over the area. For the circular orifice (1:1 ellipse aspect ratio), the orifice is meshed with 36 equal increments around the circumference and 60 approximately equal increments across each diameter. For other aspect ratios this mesh is simply stretched to achieve the correct aspect ratio, so that the number of elements remains constant. A representative mesh for the 3:1 aspect ratio orifice is shown in Figure S1(a).

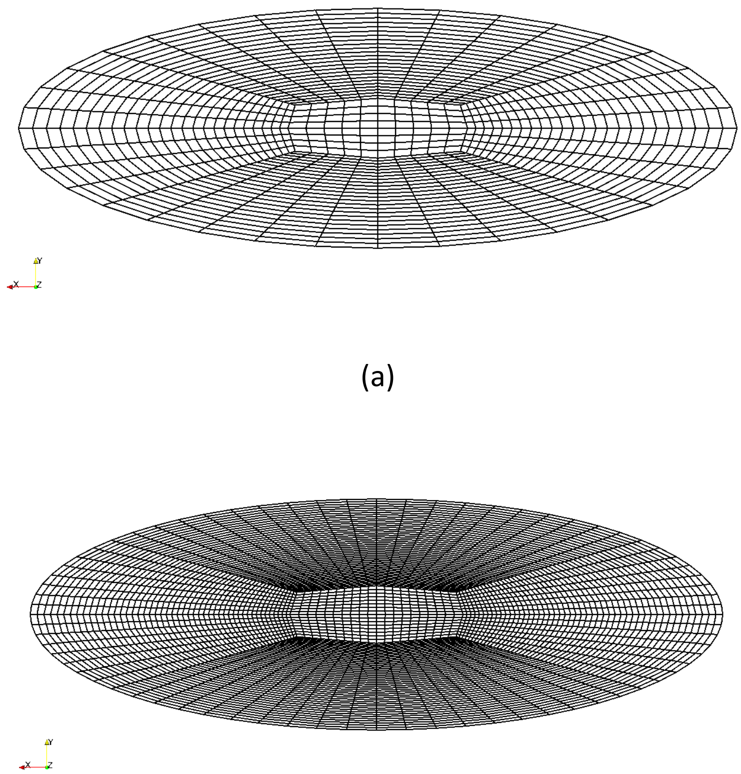

(a)

(b)

Figure S1: a) Surface mesh at orifice for the 3:1 ellipse aspect ratio geometry. The mesh on this surface comprises 944 quadrilateral elements. b) Refined mesh at orifice used for mesh refinement study. All elements in the domain (including but not limited to the orifice) are refined by a factor of 2 in all spatial dimensions.

1.6 Numerical solution

The flow is simulated using the open-source computational fluid dynamics code Nalu, which was developed by co-author Wagner and colleagues at Sandia National Laboratories. Nalu is a generalized unstructured, massively parallel flow low Mach flow solver designed to support a variety of energy applications and other research projects. In this project we take advantage of Nalu's parallel efficiency and unstructured mesh capabilities. Nalu uses a Control Volume Finite

Element Method (CVFEM) to solve the momentum and continuity equations. Further details are available in the Nalu theory manual, available online[3].

2 Solution Verification

2.1 Mesh Refinement Study

In order to ensure that the mesh used for our computation is fine enough, the case with A_O=0.3 cm^2, V_O=500 cm/s, and ellipse aspect ratio 3:1 was selected for a mesh refinement study. The original mesh for this case comprised 144,768 hexahedral elements. A refined mesh was created by halving the element size in each direction, resulting in a mesh with 8x as many elements (1,1158,144 total). The mesh at the orifice surface for the refined mesh is shown in Figure S1(b).

The modeled flow field was recomputed on the refined mesh, and the same quantities of interest were extracted as for the nominal mesh. Figure S2(a) shows the computed flow rate at the orifice relative to the true value, plotted against the distance from the orifice at which the *z* velocity is sampled. The curves are nearly indistinguishable. Figure S2(b) shows the relative difference in the two velocity solutions along the *z* axis. The difference has a peak value of around 0.65%. Because this difference is small compared to the other differences we are concerned with, we consider the original mesh size to be acceptable.

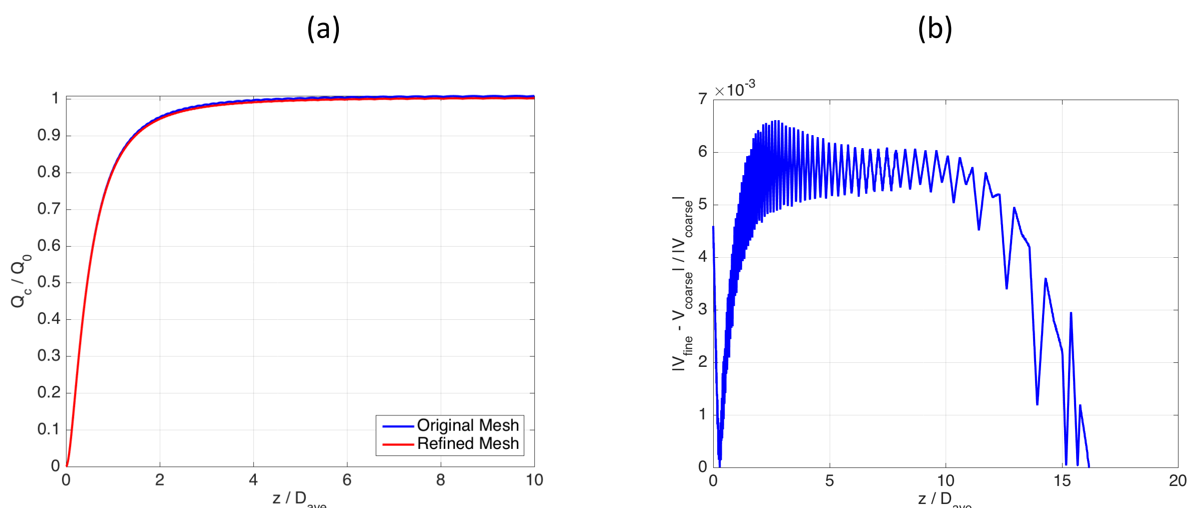

Figure S2: (a) Ratio of computed vs. actual flow rate as a function of position on the z axis where the velocity is sampled, for both the original and refined meshes. (b) Relative difference in z-velocity between original ("coarse") and refined ("fine") meshes.

[3] https://github.com/NaluCFD/Nalu

2.2 Error Estimation

We can use the coarse and fine mesh solutions, together with the knowledge that our computational formulation gives an error that is order h^2 in the element size[4], to estimate the discretization error in our solution. Using Richardson extrapolation [ref] to estimate the exact solution in terms of our coarse and fine solutions gives:

$$\mathbf{u}_{exact} = \mathbf{u}_{fine} + \frac{1}{3}(\mathbf{u}_{fine} - \mathbf{u}_{coarse}) + O(h^3)$$

The relative error with respect to this exact solution gives an estimate of the discretization error. Using this approach, we find that the maximum relative error in our velocity solution is about 0.9%, which is small compared to other errors we are concerned with in our study.

2.3 Steady State Assumption

We evolved our simulations from a zero-velocity initial condition to steady state, rather than solving for a time-dependent, pulsatile flow as is present in the real heart. Our simulations reached steady state on a timescale of about 0.001 s, indicating that responses to changes at the boundary are effectively instantaneous at scales larger than this. To test this, we have modified the boundary conditions to mimic pulsatile flow that increases to a maximum flow rate over a time of 0.1 s, i.e., the original steady boundary condition is replaced by the time-dependent condition:

$$\mathbf{u} = -\frac{Q_O \hat{\mathbf{e}}_r}{2\pi r^2}\left(\frac{1}{2} - \frac{1}{2}\cos\left(\frac{2\pi t}{T}\right)\right)$$

where T = 0.2 s is the period.

(a) (b)

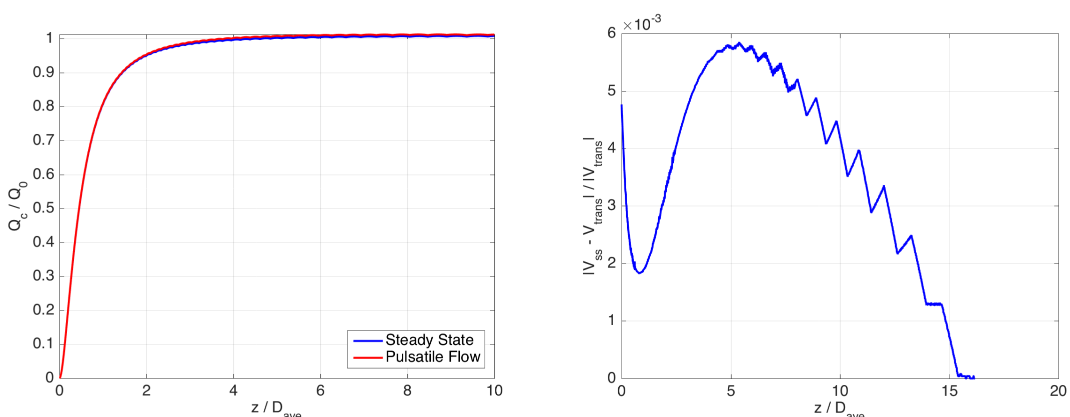

Figure S3:Comparison between steady state and pulsatile flow solutions. Pulsatile solutions are measured at the time of peak velocity. (a) Computed flow rates for the two cases, normalized by the true flow rate, as a function of z position where the velocity is sampled. (b) Relative velocity between the steady state and transient (pulsatile) cases.

---

[4] Domino, S.P. "A comparison of various equal-order interpolation methodologies using the method of manufactured solutions." *Stanford Center for Turbulence Research*, *Proceedings of the Summer Program 2008*.

The difference between the steady and pulsatile solutions at the time of maximum velocity is shown in Figure S3. The maximum difference in the velocity field is less than 0.6%, negligible compared with the differences we are concerned with.

3 Analysis and Results

3.1 Post-Processing

All 45 simulation cases were converged to a steady state solution, and final velocity and pressure at all node locations were output to files readable by the open-source visualization and post-processing software ParaView[5]. Velocity contours are plotted on specified surfaces and cross-sectional planes. For example, Figure S4 shows contours of the velocity magnitude for the simulation case with V_O=500 cm/s, orifice area A_O=0.3 cm^2, and elliptical orifice with aspect ratio 3:1. Contours are shown on cross-sectional planes in the *x*, *y*, and *z* normal directions intersecting the center of the orifice. See also manuscript Figures 2 and 3. Note that contour surfaces of constant velocity are hemi-ellipsoidal near the orifice but hemispherical farther away, supporting the hypothesis that the effect of orifice shape can be neglected when the velocity is measured far enough away from the orifice.

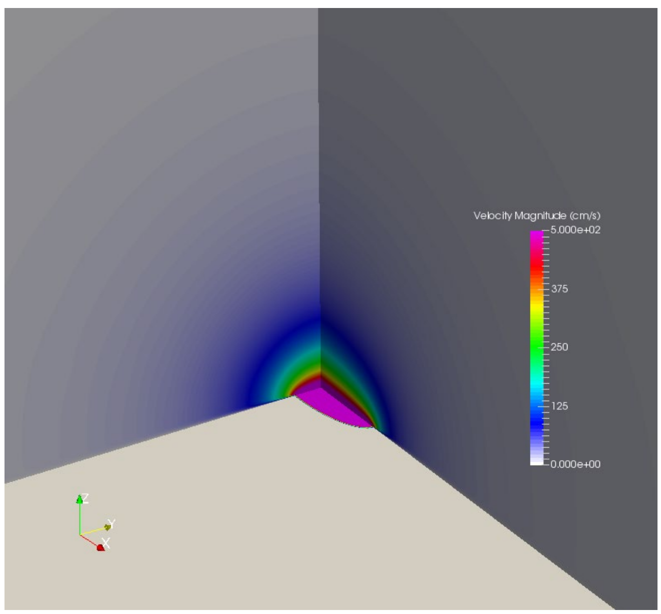

Figure S4: Velocity magnitude contours for simulation case with V_O=500 cm/s, orifice area 0.3 cm^2, and elliptical orifice with aspect ratio 3:1. Contours are shown on the x, y, and z planes.

For each simulation, the velocity field is interpolated in ParaView at points on the *z* axis at intervals of 0.005 cm, giving the velocity (and in particular the vertical component of velocity) as a function of *z* along the centerline. The magnitude of the velocity, *V*, decreases along this axis; away from the vicinity of the orifice, it is inversely proportional to the square of the

[5] https://www.paraview.org/

distance from the orifice (see Figure S5). The velocity decay is similar across a range of orifice aspect ratios.

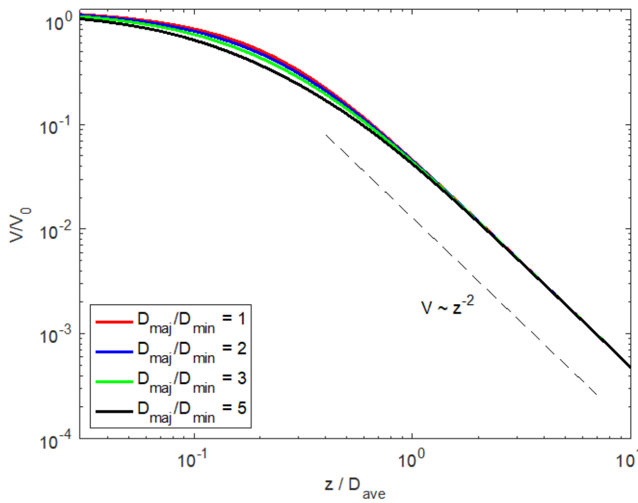

Figure S5: Normalized vertical velocity as a function of position along the z axis for varying orifice aspect ratios (V_0=400 cm/s, A_0=0.3 cm^2). The velocity decays as z^{-2} away from the vicinity of the orifice.

3.2 Flow rate calculation

At every *z* location along the centerline, the vertical velocity component V_z can be used to obtain a calculated flow rate, i.e., the flow rate that would be measured using the proximal isovelocity surface area (PISA) method for the given values of V_z and *z* (where $r=z$ is the distance to the center of the orifice). This flow rate is calculated by assuming that the given point lies on a hemispherical surface that is a contour of constant velocity magnitude equal to V_z, with velocity everywhere directed radially inward (toward the center of the orifice):

$$Q_C(z) = 2\pi z^2 V_z(z)$$

where the dependence of both Q_C and V_z on *z* has been made explicit. The calculated value of flow rate can be compared to the true flow rate Q_O for each simulation and at each *z* location. If contour of constant velocity magnitude truly is hemispherical at a given distance from the orifice, the ratio between Q_C and Q_O should be one. Figure 5 in the manuscript, reproduced as Figure S6 below, shows this ratio as a function of *z* for all simulations with orifice aspect ratio 1:1 and 5:1. In this plot, the *z* coordinate is normalized by the geometric mean diameter $D_{ave}=(4A_O/\pi)^{1/2}=(D_{maj}D_{min})^{1/2}$, where D_{maj} and D_{min} are the major and minor diameters of the elliptical orifice. This ratio of computed to actual flow rate does indeed approach one for large enough distances from the orifice

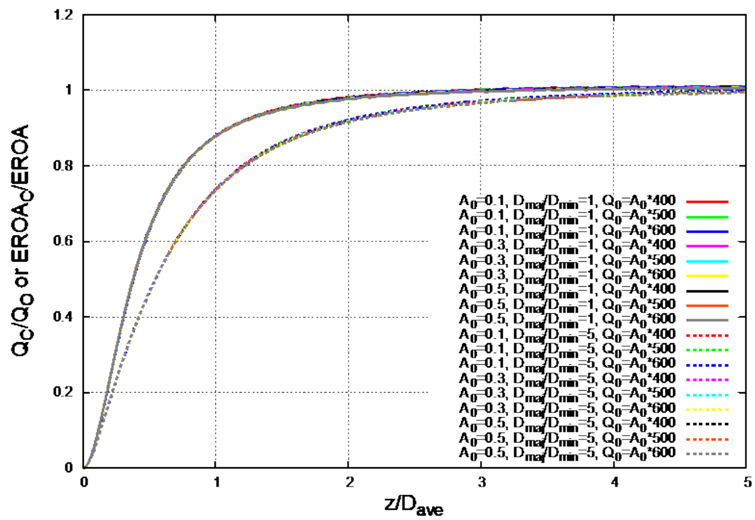

Figure S6: (Figure 5 in manuscript) Computed hemispherical flow rate (Qc) and effective regurgitant orifice area (EROAc), normalized by true flow rate (Qo) and effective regurgitant orifice area (EROA), respectively, plotted against contour distance normalized by the geometric mean diameter $D_{ave}=(D_{maj}D_{min})^{1/2}$, where D_{maj} and D_{min} are the major and minor diameters of the elliptical orifice. Data is plotted for two different ellipse axis ratios (1:1 and 5:1) and various values of true orifice area A_O and true flow rate Q_O. (z = distance from proximal isosurface from regurgitant orifice).

The effective regurgitant orifice area ($EROA_C$) can also be calculated at each z location by assuming that the outflow velocity measured at the orifice, V_O, is constant across the orifice, and that the total flow rate is therefore equal to $V_O A_O$:

$$\mathrm{EROA}_C = \frac{Q_C}{V_O} = \frac{2\pi z^2 V_z}{V_O}$$

The ratio between the calculated and true effective areas is equivalent to the ratio between the calculated and true flow rates, as noted in Figure S6.

It is clear from Figure S6 that the PISA method leads to an underestimation of the true effective area, and that this underestimation is larger for a non-circular orifice than for the circular case. Because our goal is to assess the effect of a non-circular orifice on the effective area (or flow rate) estimation, a quantity of interest is the amount of underestimation *relative* to what would be computed for a circular orifice; this represents the additional error due to non-circularity. If the flow rate computed for a circular orifice is Q_{circ}, then the relative underestimation is

$$\frac{Q_{circ} - Q_C}{Q_{circ}} = \frac{V_{z,circ} - V_z}{V_{z,circ}}$$

where $V_{z,circ}$ is the flow velocity that would be measured for a circular orifice of the same area at the same z location; $V_{z,circ}$ is obtained from our simulations of an orifice with 1:1 aspect ratio. This quantity is plotted in Figure 5 of the manuscript as a function of V_z/V_O, which is a parameter that can be calculated from measured data during clinical application of the PISA method.